Analytical and Numerical Solutions for Natural Convection in a Corner

Paolo Luchini*
University of Naples, Naples, Italy

Laminar natural convection flow in a corner delimited by a vertical heated semi-infinite plate and a second room-temperature plate forming an arbitrary angle is studied both analytically and numerically. Analytically, repeated use of the matched asymptotic expansions technique shows that the boundary layer along the vertical plate is described, to first order, by Polhausen's classical similarity solution; this buoyancy-induced flow drives an outer irrotational flow which, in turn, provides the motive force for a self-similar viscous boundary layer along the second plate. In the numerical approach, a variable-spacing, finite difference method with dynamic mesh modification permits a solution of the Navier-Stokes equations to be obtained in the whole field, confirming the validity of the approximate analytical model.

I. Introduction

PRESENTLY, natural convection is well in the core of basic fluid dynamic research, with several papers being published each year; see, for example, the 1984 Annual Review of the *International Journal of Heat and Mass Transfer*.[1]

One main issue in this field is the buoyant flow excited by a heated vertical plate. Although research on this problem can be tracked as far back as 1881,[2] only in the 1930s was it posed in a proper frame when Polhausen found his classical similar boundary-layer solution.[3] Since then many researchers have studied, and are still studying, different aspects of this problem, e.g., transient behavior,[4,5] the effect of simultaneous mass and heat transfer,[6,7] interaction with forced convection,[8] finite-plate[9-12] or inclined-plate[13] situations, and flow through porous media.[14]

This paper deals with the flow existing in a corner formed by two semi-infinite plates (one of which is vertical and heated above room temperature), with particular regard to the flow that develops outside the buoyant boundary layer next to the vertical wall. The outer flow generated by a buoyant boundary layer was studied in the past for the case of a semi-infinite or finite heated vertical plate isolated in free space. Yang and Jerger[9] addressed this problem for a vertical finite plate to generate higher-order boundary-layer corrections to Polhausen's solution; in fact, the first boundary-layer correction is coupled to the first nonzero outer approximation. Their work was extended by Kierkus[13] who considered an inclined plate, showing that the difference between forward and backward inclination appears in the second boundary-layer approximation. Yang and Jerger's work was later criticized by Clarke,[15] who argued that they did not account properly for plate finiteness and gave the outer solution for a semi-infinite vertical plate; Kierkus' paper was criticized similarly by Riley,[16] who studied the flow generated by a semi-infinite inclined plate.

All of these papers dealt with a heated vertical plate isolated in free space. The corner problem does not seem to have been analyzed previously.

Natural convection in such a geometry, for the particular case of a 90-deg corner, has been studied experimentally in Ref. 17, measuring the heat transfer from the wall. The results presented therein are in good agreement with the classical boundary-layer theory[3]; in fact, as also appears in the present paper, heat-transfer phenomena are limited to the vertical boundary layer and are influenced only at higher orders of approximation by the presence of the second wall, which, on the other hand, has a zeroth-order effect on fluid motions outside the thermal boundary layer.

The present theoretical study starts from the two-dimensional Navier-Stokes equations with the Boussinesq approximation.

For the approximate analytical solution, by repeated use of the inner-outer technique, several regions are identified in which different approximations are valid, in a sequel starting from the vertical boundary layer. Preliminary results of this analysis are contained in Ref. 18.

For the numerical solution, a self-adapting, variable-spacing, finite difference method devised by the present author[19] is adopted. Indeed, a variable-spacing method is necessary to solve the Navier-Stokes equations for two reasons: the presence of rapid variation regions, which require a fine mesh, together with slow variation regions, where a much coarser mesh is sufficient, and the infinity of the solution domain, which requires truncation along a suitably far line and use of a larger and larger mesh approaching this line. The adopted method dynamically generates the mesh during the calculation, finding the proper size in each region automatically. The good agreement observed between the numerical solution, performed for a 90-deg corner, and the approximate analytical solution attests to the validity of the approximation.

II. Equations and Boundary Conditions

A domain bounded by two semi-infinite plates forming an angle φ_0 between them (one being vertical and heated at a temperature t_1 and the other inclined and at room temperature t_0) is considered (see Fig. 1).

The equations describing the steady, thermofluiddynamic field in this domain in the Boussinesq approximation are, in dimensionless form,

$$\operatorname{div} V = 0 \tag{1a}$$

$$V \cdot \operatorname{grad} V + \operatorname{grad} p = \Delta_2 V + T\hat{x} \tag{1b}$$

$$V \cdot \operatorname{grad} T = (1/P)\Delta_2 T \tag{1c}$$

where P is the Prandtl number and $\hat{x}$ is a unit vector in the vertical (x) direction; T is the temperature difference from room temperature nondimensionalized with respect to $\Delta t_r = t_1 - t_0$; the reference length is $L_0 = (\nu^2/g\beta\Delta t_r)^{1/3}$, where

Received April 30, 1985; revision submitted July 20, 1985.

*Ricercatore, Istituto di Gasdinamica, Facoltà di Ingegneria.

ν denotes the kinematic viscosity, g the gravity acceleration, and β the thermal expansion coefficient; the reference velocity is $V_0=\nu/L_0$ and p, the pressure difference from hydrostatic pressure, is nondimensionalized with respect to $p_0=\rho V_0^2$.

The formulation of Eqs. (1) in terms of stream function ψ and vorticity ω, which we shall also adopt, can be obtained by defining ψ so that $\psi_x=-v$ and $\psi_y=u$ (u and v being the velocity components along the x and y axes) and $\omega=u_y-v_x$. Then Eqs. (1a) and (1b) can be superseded by

$$\Delta_2\psi=\omega \tag{1d}$$

$$V\cdot\mathrm{grad}\omega=\Delta_2\omega+T_y \tag{1e}$$

The boundary conditions are $T=1$ on the vertical wall, $T=0$ on the second wall, and $V=0$ on both walls.

It is important to observe that no characteristic length is defined by the geometry of this problem; therefore, a Reynolds or Grashof number cannot be constructed with absolute meaning. Although we shall find it useful to introduce a local Grashof number in the analytical approach, it should not be forgotten that the basic equations of the problem, Eqs. (1), depend on one parameter only—the Prandtl number.

III. Analytical Approach

Identification of Subregions

In the solution of the present problem several subregions with different behaviors can be recognized (Fig. 2). First, the flow presents a completely different character at a distance from the corner very large or very small compared to the characteristic length L_0, i.e., much greater or much less than unity in the dimensionless formulation of Eqs. (1). Second, the region far from the corner can be further subdivided into two boundary layers close to the walls and an irrotational outer region.

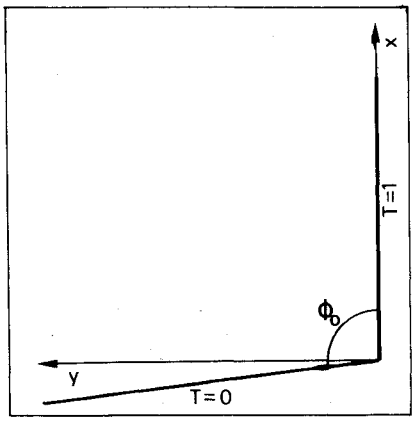

Fig. 1 Geometry of the problem.

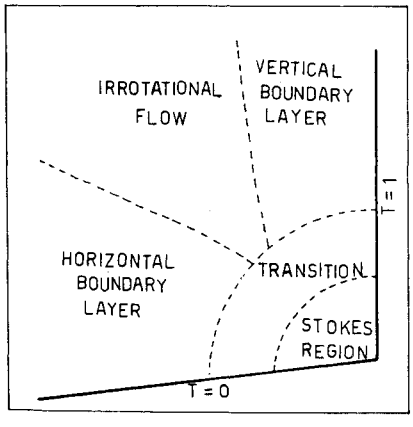

Fig. 2 Regions of different behavior.

To show the existence of these regions, we introduce a suitable rescaling of variables for each of them, after which a small parameter appears multiplying some of the terms of Eqs. (1) and an approximation becomes possible. In particular, to study the region close to the corner, with a size small compared to L_0, a fictitious reference length $L\ll L_0$, a new reference velocity $(L/L_0)^2V_0$, and a new reference pressure $(L/L_0)p_0$ are adopted, thus obtaining the equations

$$\Delta_2 V+T\hat{x}-\mathrm{grad}p=(L/L_0)^3V\cdot\mathrm{grad}V \tag{2a}$$

$$\Delta_2 T=(L/L_0)^3PV\cdot\mathrm{grad}T \tag{2b}$$

which for small $(L/L_0)^3$ reduce to the Stokes equations.

To study the far region, at a distance from the corner much greater than L_0, a reference length $L\gg L_0$ is introduced, adopting a new reference velocity $(L/L_0)^{1/2}V_0$ and a new reference pressure $(L/L_0)p_0$. Thus, we obtain the equations

$$V\cdot\mathrm{grad}V+\mathrm{grad}p-T\hat{x}=(L_0/L)^{3/2}\Delta_2 V \tag{3a}$$

$$V\cdot\mathrm{grad}T=(L_0/L)^{3/2}\Delta_2 T/P \tag{3b}$$

which for small $(L_0/L)^{3/2}$ reduce to the Euler equations.

As is known, since substituting Eqs. (3) with the Euler equations the highest-order derivatives are lost, this approximation is not uniformly valid and boundary layers must be introduced near the walls. To obtain the equations for the boundary layer near the vertical wall, we consider L and $(L/L_0)^{1/2}V_0$ as the reference length and velocity only in the x direction, and $L^{1/4}L_0^{3/4}$ and $(L_0/L)^{1/4}V_0$ as the reference length and velocity in the y direction, thus finding

$$uu_x+vu_y+p_x-T-u_{yy}=(L_0/L)^{3/2}u_{xx} \tag{4a}$$

$$p_y=(L_0/L)^{3/2}(v_{yy}-uv_x-vv_y)+(L_0/L)^3v_{xx} \tag{4b}$$

$$uT_x+vT_y-T_{yy}/P=(L_0/L)^{3/2}T_{xx}/P \tag{4c}$$

To analyze the other boundary layer, the orientation of the reference frame must be changed so that one of the axes lies along the second wall.

Having so redefined the axes, the reference lengths and velocities for this region must be taken as L and $(L_0/L)^{1/4}V_0$ for the longitudinal (x) direction and L_0 and $(L_0/L)^{5/4}V_0$ for the normal (y) direction. The resulting equations are

$$uu_x+vu_y+p_x-u_{yy}=(L_0/L)^{1/2}T+(L_0/L)^{3/2}u_{xx} \tag{5a}$$

$$p_y=(L_0/L)^{3/2}(v_{yy}-uv_x-vv_y)+(L_0/L)^3v_{xx} \tag{5b}$$

$$uT_x+vT_y-T_{yy}/P=(L_0/L)^{3/2}T_{xx}/P \tag{5c}$$

The approximations afforded by Eqs. (2-5) must be properly matched to each other to determine the boundary conditions for each region. The coupling between the boundary layers and the irrotational region can be realized by means of the classical theory of matched asymptotic expansions. On the contrary, this theory cannot be applied to the coupling of the Stokes region with the others because of the lack of a region where both approximations are simultaneously valid. Instead a region exists, indicated in Fig. 2 as the transition region, where neither approximation holds, because all of the terms in Eqs. (1) are of the same order of magnitude. However, it must be noticed that this transition region is located at a distance from the corner of the order of L_0 and, assuming for instance $\nu^2/g\beta=10^{-8}$ m^3-K (air), one has $L_0\simeq 0.5$ mm for $\Delta t_r=100$ K and $L_0\simeq 2$ mm for $\Delta t_r=1$ K. Therefore, the transition and Stokes regions have a very

small extension and their existence can be neglected in many applications.

Vertical Boundary Layer

By expanding in Eqs. (4) each unknown f in a series of the form[20]

$$f(x,y,\epsilon)=\sum_{i=1}^{\infty}\delta_i(\epsilon)f_i(x,y) \tag{6}$$

where $\epsilon=(L_0/L)^{3/2}$ and $\lim_{\epsilon\to 0}\delta_{i+1}/\delta_i=0$, at leading order the Prandtl boundary-layer equations are obtained.

The standard application of the matched asymptotic expansions technique, for instance to forced flat-plate flow, requires the irrotational outer flow to be determined first and is then used to give boundary conditions to the boundary layer. In the free convection case, contrary to the forced convection case, the irrotational region must be considered at rest in the first approximation. As a consequence, the vertical boundary-layer equations must be solved with a condition specifying zero outer velocity, and are not affected at the first approximation by the existence of other bodies such as the second wall. Therefore, the boundary conditions to be associated with the vertical boundary-layer equations are: $u(x,0)=v(x,0)=0$, $T(x,0)=1$, $u(x,\infty)=T(x,\infty)=0$, $u(0,y)=T(0,y)=0$, and the well-known similar solution[3] is obtained in the form

$$u=x^{1/2}F_1'(z),\quad T=G_1(z),\quad z=y/x^{1/4} \tag{7}$$

In particular for $P=0.71$: $u_y(x,0)=F_1''(0)x^{1/4}=0.958x^{1/4}$, $T_y(x,0)=G_1'(0)x^{-1/4}=-0.355x^{-1/4}$, and $v(x,\infty)=-[3F_1(\infty)/4]x^{-1/4}=-1.264x^{-1/4}$.

Notice that L was introduced in Eqs. (4) only as an expansion parameter in order to find an approximation valid on a length scale that was large compared to L_0; since the value of L has not been specified, the resulting solution, Eq. (7), is valid for any L. Now that the solution has been obtained, it is convenient, for the purpose of matching the different regions, to set $L=L_0$, i.e., to go back to the variables used in Eqs. (1).

Irrotational Region

By expanding each unknown in Eqs. (3) in a series similar to Eq. (6), an approximation valid in the region far from both walls is obtained.

Choosing the coefficients $\delta_2(\epsilon)$ for velocity (δ_{2V}), pressure (δ_{2p}), and temperature (δ_{2T}) so that the greatest possible number of terms of Eqs. (3) are of the same order in ϵ, one obtains the relations $\delta_{2p}=\delta_{2T}=\delta_{2V}^2$ and Eqs. (3) reduce to the Euler equations in the leading (second) approximation.

In the ψ,ω formulation, the Euler equations are

$$\Delta_2\psi=\omega \tag{8a}$$

$$V\cdot\mathrm{grad}\omega=T_y \tag{8b}$$

$$V\cdot\mathrm{grad}T=0 \tag{8c}$$

Equation (8c) gives a constant temperature along each streamline; since $T=0$ at infinity, $T=0$ everywhere. Then Eq. (8b) yields a constant vorticity along each streamline, and by the same argument we find that $\omega=0$ identically. This region is therefore irrotational.

To find the boundary conditions for Eq. (8a) we observe that we are calculating what would normally be the second approximation to the outer region (in the present case the first approximation is zero). That is why this region must be analyzed after the boundary layers are analyzed. In particular, on the vertical wall the normal velocity must be imposed to equal the asymptotic value resulting from the boundary layer. Using once again the primitive scaling of Eqs. (1), from Eq. (7) the condition descends to $\psi(x,0)=F_1(\infty)x^{3/4}$ [where, for example, for $Pr=0.71$, $F_1(\infty)=1.685$]. On the second wall, where no heat source exists, the boundary-layer solution corresponding to a null outer velocity is identically zero, and the normal velocity for the second outer approximation must be imposed to vanish.

To summarize: To find the leading term of the outer expansion one must solve the Laplace equation, $\Delta_2\psi=0$, with the conditions $\psi=F_1(\infty)x^{3/4}$ on the vertical wall and $\psi=0$ on the second wall. To complete the statement of this problem, the behavior of ψ at infinity must also be assigned. The correct choice of this behavior is not trivial, because ψ is required to go to infinity at $x^{3/4}$ along the vertical wall. Taking into account that, in reality, the infinite plate models a very long but finite plate the solution that is interesting from a physical point of view is the one obtained by limiting the heating to a finite length and then, after having found the solution, letting this length go to infinity. To this end it is useful to express the solution as follows, using Green's function G:

$$\psi(x,y)=-\int_0^{\infty}\psi(x_1,0)G_{y_1}(x,y,x_1,0)\,dx_1 \tag{9}$$

where Green's function for a corner of angle φ_0 is

$$G=\frac{1}{2\pi}\log\left|\frac{z_1^a-z^a}{z_1^a-\bar{z}^a}\right|$$

with $z=x+iy$, $\bar{z}=x-iy$, $z_1=x_1+iy_1$, and $a=\pi/\varphi_0$. As

$$G_{y_1}(x,y,x_1,0)=\frac{1}{2\pi}\frac{\mathrm{Im}(z^a)ax_1^{a-1}}{x_1^{2a}-2\mathrm{Re}(z^a)x_1^a+|z|^{2a}}$$

we obtain that the integral of Eq. (9) is convergent only if $\psi(x,0)/x^a$ vanishes at infinity. In particular, for $\psi\propto x^{3/4}$, the condition $a>3/4$ implies $\varphi_0<4\pi/3$, so that the solution exists only for an angle smaller than this limit. In other words, when $\varphi_0\geq 4\pi/3$ it is not possible to approximate a long but finite heated plate using an infinite one, because in the limiting process of letting the plate length go to infinity the whole solution becomes infinite.

The solution, in the range where it exists, can be found without explicitly calculating the integral of Eq. (9) by simply noticing that the complex analytic function which reduces to $x^{3/4}$ on the x axis is $z^{3/4}$. Multiplying this by the coefficient $e^{-i3\varphi_0/4}$, one obtains a function whose imaginary part vanishes for $\varphi=\varphi_0$. Therefore, the solution is

$$\psi=F_1(\infty)\mathrm{Im}[e^{-i3\varphi_0/4}z^{3/4}]/\sin(-3\varphi_0/4)$$

that is, in polar coordinates

$$\psi=F_1(\infty)r^{3/4}\sin|3(\varphi-\varphi_0)/4|/\sin(-3\varphi_0/4) \tag{10}$$

For $\varphi_0\to 4\pi/3$, ψ is infinite, as expected; for $\varphi_0>4\pi/3$, Eq. (10) yields a solution of the problem devoid of physical meaning.

According to Eq. (10), the longitudinal velocity V_1 at the second wall is

$$V_1=-3F_1(\infty)r^{-1/4}/4\sin(3\varphi_0/4) \tag{11}$$

the minus sign denotes that the flow is directed toward the corner.

The longitudinal velocity u at the vertical wall is

$$u=-3F_1(\infty)x^{-1/4}/4\tan(3\varphi_0/4)$$

and is much smaller than in the boundary layer (where it is proportional to $x^{1/2}$), as can be expected since it is a second

approximation. Notice that the outer longitudinal velocity at the vertical wall is directed toward the corner for angles φ_0 less than $2\pi/3$ and away from the corner for angles greater than this limit.

Secondary Boundary Layer

Due to the flow induced in the outer irrotational region a boundary layer also develops on the second wall.

By expanding each unknown in Eqs. (5) in a series similar to Eq. (6), the equations valid in the secondary boundary-layer region are obtained. [Recall that x,u and y,v have been redefined for the scope of Eqs. (5) to be parallel and normal, respectively, to the second wall.] At the leading approximation, the Prandtl boundary-layer equations are obtained; again letting $L=L_0$, the boundary conditions are the following: $u(x,0)=v(x,0)=T(x,0)=0$, $u(x,\infty)=-U_0x^{-1/4}$, and $T(x,\infty)=0$, where $U_0=3F_1(\infty)/4\sin(3\varphi_0/4)$ is the longitudinal velocity imposed by the outer region.

No condition is given at $x=0$, because this is a singular point of the solution. Instead of specifying such a condition, it is imposed that the solution be similar, on the basis that no characteristic length exists in this boundary layer which could justify a nonsimilar solution. Thus, we find that

$$T(x,y)=0, \quad u(x,y)=x^{-1/4}F_2'(z), \quad z=y/x^{5/8} \tag{12}$$

where F_2 is the solution of

$$F_2'''=(U_0^2-F_2'^2)/4-3F_2F_2''/8 \tag{13}$$

with the conditions $F_2(0)=F_2'(0)=0$ and $F_2'(\infty)=-U_0$. U_0 can be eliminated from Eq. (13) by letting $F_2(z)=-U_0^{1/2}F_3(U_0^{1/2}z)$, where the function $F_3(z)$, independent of U_0, obeys the equation

$$F_3'''=(F_3'^2-1)/4+3F_3F_3''/8$$

with the conditions $F_3(0)=F_3'(0)=0$, $F_3'(\infty)=1$.

A plot of $F_3'(z)$, obtained by numerical integration, is drawn in Fig. 3. The friction coefficient $u_y(x,0)$ is

$$u_y(x,0)=-F_3''(0)U_0^{3/2}x^{-7/8}$$

$$=-0.529[3F_1(\infty)/4\sin(3\varphi_0/4)]^{3/2}x^{-7/8} \tag{14}$$

and depends on the Prandtl number through the factor $F_1(\infty)^{3/2}$ and on the angle φ_0 through the factor $\sin^{-3/2}\times(3\varphi_0/4)$.

Characteristic of this region is the unusual shape of the boundary layer, whose thickness decreases in the streamwise direction, losing fluid to the outer region.

It is interesting in this respect to follow a streamline in its path through the three convective regions, which are all located at a distance from the corner much greater than L_0. A generic streamline originates in the secondary boundary layer, following a line $y=\text{const}\cdot x^{7/16}$ at infinity (x and y being chosen parallel and normal to the second wall, respectively). Then it crosses the outer edge of the boundary layer and enters the irrotational region along a line $y=\text{const}\cdot x^{1/4}$.

In the outer region the streamline bends downward and eventually approaches the vertical wall at an angle $3\varphi_0/4$, greater or smaller than $\pi/2$ depending on whether $\varphi_0\gtrless 2\pi/3$. Once in the vertical boundary layer, the streamline bends rapidly upward, finally going to infinity along a line $y=\text{const}\cdot x^{-1/8}$ (where x and y are now parallel and normal to the vertical wall).

A typical streamline is given in Fig. 4 for an angle $\varphi_0=\pi/2$.

Notice that no thermal effects are present out of the vertical boundary layer, therefore, the thermal behavior of the second wall (e.g., whether it is isothermal or adiabatic) is unimportant. This is true even in the higher-order boundary-layer approximations, because temperature becomes exponentially small out of the thermal boundary layer.

Stokes Region

At a distance from the corner that is small compared to L_0, Eqs. (2) must be used, which reduce to the Stokes equations at leading order.

The boundary conditions are $T=1$ on the vertical wall, $T=0$ on the second wall, and $V=0$ on both walls.

The most general regular solution of this linear problem can be expressed in polar coordinates r and φ, in terms of the stream function ψ, as

$$T=g(\varphi)+\Sigma A_i r^{a_i}g_i(\varphi) \tag{15a}$$

$$\psi=r^3f(\varphi)+\Sigma A_i r^{a_i+3}f_i(\varphi)+\Sigma B_i r^{b_i}h_i(\varphi) \tag{15b}$$

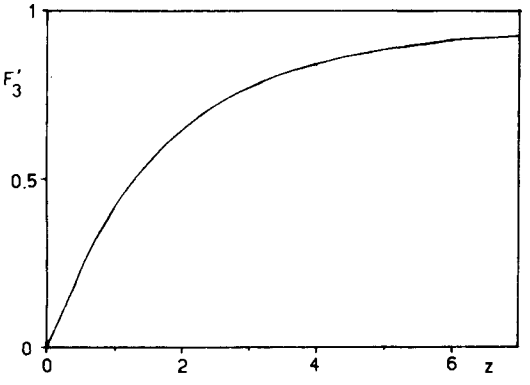

Fig. 3 Plot of the second boundary-layer velocity $F_3'(z)$.

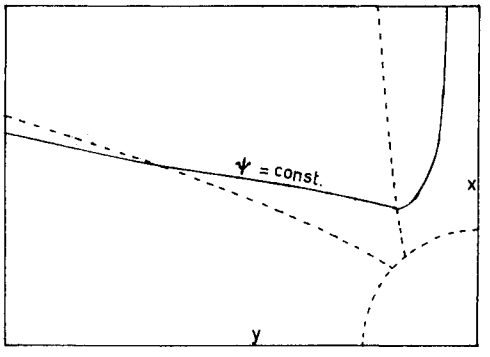

Fig. 4 Typical streamline for $\varphi_0=\pi/2$.

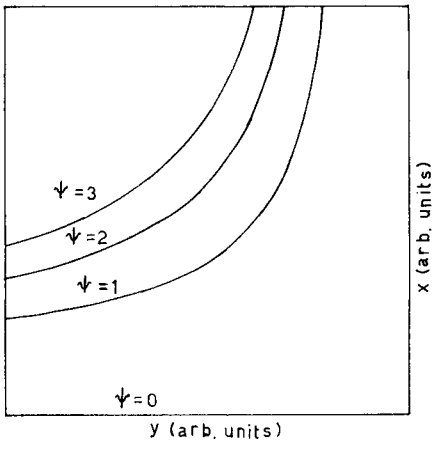

Fig. 5 Streamline pattern for the solution of the Stokes equations ($\varphi_0=\pi/2$).

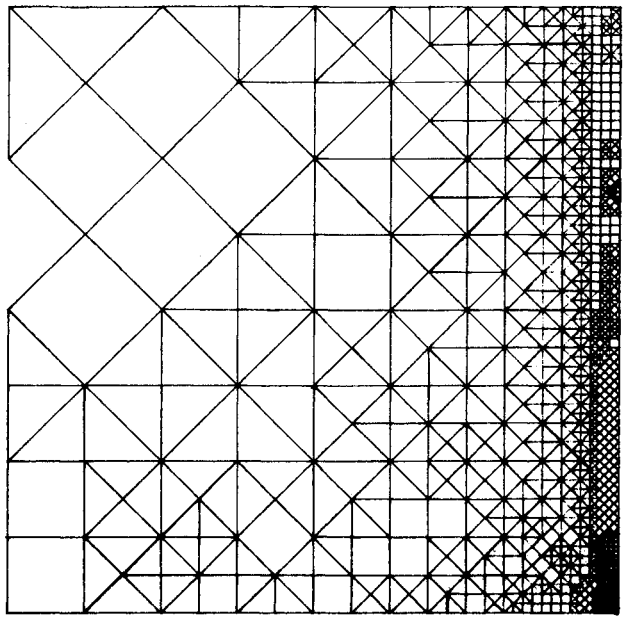

Fig. 6 Calculation grid for a 100×100 square.

where a_i and b_i are positive, generally noninteger exponents and A_i and B_i arbitrary coefficients. Notice, however, that the expansion in terms of L/L_0 is actually an expansion in terms of r, because at any distance from the corner one can always set either L equal to that distance and r equal to one, or vice versa. For this reason only the term with the lowest power of r in Eqs. (15) must appear in the leading approximation, and all of the A_is and B_is must be set equal to zero.

To determine g and f we observe that the Laplacian of a function of the form $r^a F(\varphi)$ is $r^{a-2}(F''+a^2F)$, and the Stokes equations in ψ-ω form, $\Delta_2\psi=\omega$, $\Delta_2\omega=T_y$, $\Delta_2 T=0$, reduce to the ordinary equations

$$g''=0, \quad h''+h=-g'\cos\varphi, \quad f''+9f=h \tag{16}$$

where $\omega=rh(\varphi)$, with boundary conditions $g(0)=1$, $g(\varphi_0)=0$, and $f(0)=f'(0)=f(\varphi_0)=f'(\varphi_0)=0$. The solution of the first equation is $g=1-\varphi/\varphi_0$. The solution of the second equation is then $h=(\varphi/2\varphi_0)\sin\varphi+C_1\sin\varphi+C_2\cos\varphi$, where C_1 and C_2 cannot be determined before solving the third equation. Finally, the expression of f results to be

$$16f=(\varphi/\varphi_0)\sin\varphi+[(1/\sin^2\varphi_0-\cot\varphi_0/\varphi_0-2)\sin\varphi + (1/\varphi_0-2\cot\varphi_0)\cos\varphi]\sin^2\varphi \tag{17}$$

The resulting streamline pattern for $\varphi_0=\pi/2$ is shown in Fig. 5.

Finally, we note that if the second wall is assumed to be adiabatic rather than isothermal, the temperature must be constant everywhere in this region at the leading approximation so that no buoyancy-induced flow exists at leading order and the first nonzero term in the expansion of ψ comes from coupling with the far region. This coupling, however, is not easy to calculate because an overlap region where both the Stokes and convective approximations are simultaneously valid does not exist. On the contrary, a transition region occurs, represented in Fig. 2 at a distance of order L_0, where only the full Navier-Stokes equations apply.

IV. Numerical Approach

Calculation Method

To solve the Navier-Stokes equations numerically [Eqs. (1)] for the present problem, several difficulties must be overcome, the foremost of which are the presence of regions characterized by a markedly different behavior of the flow, already put in evidence by the previous analysis, and the infinity of the integration domain. To handle this situation a variable-spacing method is necessary in order to have a finer mesh in the boundary layers where the gradients are higher, together with a coarser mesh in the outer region, and a general increase of the mesh size approaching infinity.

The particular method chosen, developed by the present author, is also self-adapting, modifying dynamically the distribution of mesh points during the calculation on the basis of the evolving solution.

This method, only a brief sketch of which will be given in the following, is described in Ref. 19. At its basis is a mesh-management algorithm which adds or deletes single points from the mesh in such a manner that each point is always the center of a symmetrical cross formed with four other points.

Contrary to most variable-spacing schemes in the literature, the method presented herein is not based on a coordinate transformation and the mesh points are not ordered along coordinate lines. This choice has the advantage that points can be added to or deleted from the mesh singularly and a local refinement does not require a global readjustment.

The addition-deletion process is automatically performed under control of a routine determining whether or not the size of each cross is adequate on the basis of the magnitude of the second derivatives of the unknowns.

The equations in the ψ-ω form [Eqs. (1c-1e)] are discretized over each cross using upwind-weighted central differences for all of the first derivatives; to solve these equations a false-transient explicit method is adopted using a local equivalent time step adjusted at each point at the stability limit and a special form of the convective terms to extend this limit.

An explicit method is chosen because a totally implicit method, requiring the inversion of a large matrix at each iteration step, does not seem convenient in false-transient calculations, where the precise evolution of the unknowns at intermediate time steps is not relevant, and a partially implicit method (for example, alternating direction implicit) is not immediately applicable to our variable-spacing mesh due to the lack of coordinate lines.

As given in Sec. II, the boundary conditions for the present problem are $T=1$ and $V=0$ on the vertical wall and $T=0$ and $V=0$ on the second wall. In discretizing these boundary conditions, two difficulties must be overcome: 1) the nonrectangular shape of the domain, whose contour does not pass exactly through mesh points, and 2) its infinity, which requires a cut of the domain itself and the imposition of suitable truncation conditions.

Mesh points not falling exactly on the boundary can be handled using interpolation formulas; however, in the present analysis we shall consider only the case $\varphi_0=90$ deg, in which the second wall is horizontal. The temperature condition on the walls is thus immediately imposed; the discretized form of the velocity condition can be expressed in terms of the variables ψ,ω transforming the no-slip condition to a condition for ω by means of the Thom formula.[21]

The problems posed by the infinity of the solution domain deserve a longer discussion.

To cope with infinity two routes are possible: truncating the domain along a fake boundary far enough from the origin, or mapping it onto a finite one by a coordinate transformation. It must be noticed, however, that a coordinate transformation does not eliminate the need to introduce truncation boundary conditions based on the asymptotic behavior of the solution, as the infinity of the original domain is mapped into a singularity that must be excluded from the numerical calculation. Therefore, a coordinate transformation is not useful in connection with our self-

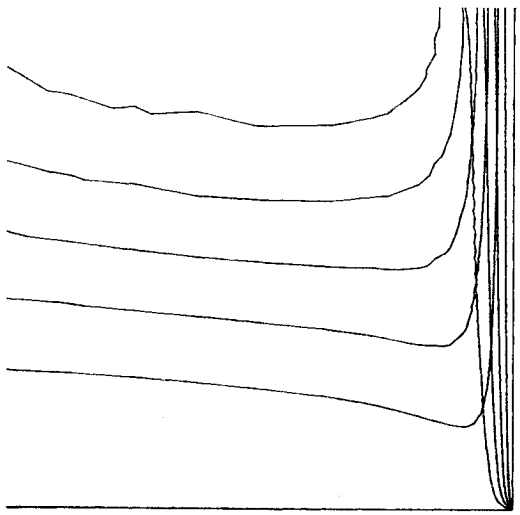

Fig. 7 Streamlines and isothermal lines for $L = 100$.

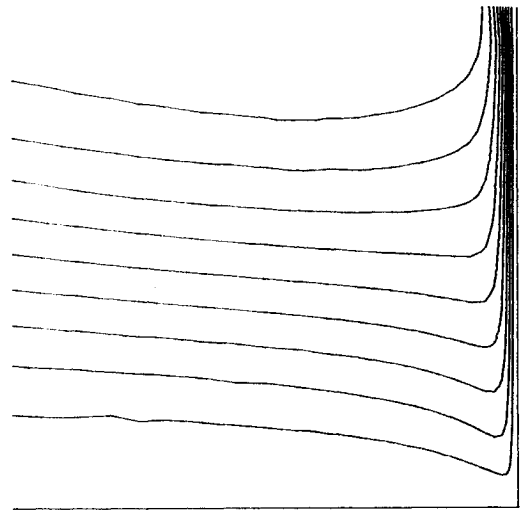

Fig. 9 Streamlines for $L = 500$.

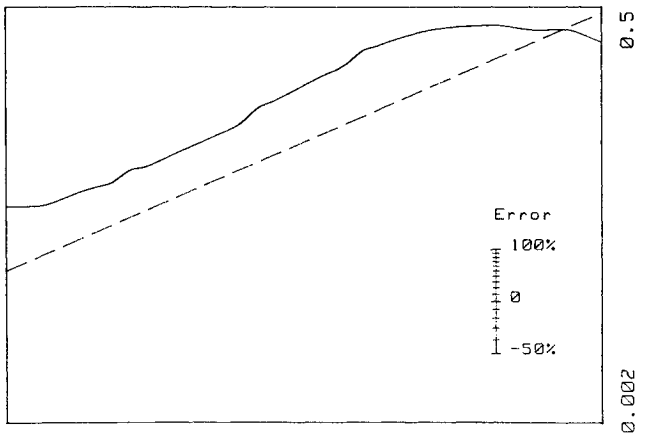

Fig. 8 Bilogarithmic plot of the second wall skin friction for the case $L = 100$, together with the boundary-layer solution (broken line).

adapting grid, which by itself can grow wider and wider while approaching infinity.

Giving the appropriate truncation conditions is a most delicate aspect because even in the statement of the analytical problem it is difficult to assign conditions at infinity such that one, and only one, solution exists; in the approximate analytical solution we have adopted for each region conditions specialized for the particular approximation, but the behavior at infinity characteristic of the various regions is difficult to put together. In fact, in the vertical boundary layer velocity is diverging at infinity, while in the other regions it is vanishing. On the other hand, in the outer region the analysis performed using Green's function showed that even the condition of vanishing velocity is not sufficient for a generic angle φ_0 (even if it is sufficient for $\varphi_0 = \pi/2$) to identify the physically significant solution, and for $\varphi_0 \geq 4\pi/3$ a solution of the infinite problem does not exist at all; for the second boundary layer we have not specified explicit conditions at infinity, but rather given them implicitly, by imposing that the solution be similar, on the assumption that the similar solution represents the limit of the boundary layer formed on a finite plate when the leading edge goes to infinity.

Because of the peculiar character of the vertical boundary layer, different numerical truncation conditions must be given for this and the other regions. The boundary-layer edge must be itself determined during the calculation, and we put it at the point of the boundary where the direction of velocity changes from inward to outward.

Even in the region out of the vertical boundary layer it is not possible to assume as a truncation condition $V = 0$ because, as shown by the analytical approach, velocity in the outer region vanishes at infinity only as $r^{-1/4}$. In addition, the condition imposing the vanishing of the normal derivatives of the three unknowns leads to a too large distortion of the flowfield. By relying on the previous analysis of the irrotational outer region, we impose the vanishing of the directional derivatives of the three unknowns along the direction of the theoretical streamlines in the part of the boundary where velocity is directed inward, preserving the vanishing-normal-derivatives condition for the region where velocity is directed outward.

Analysis of the Results

The numerical calculation was performed for $\varphi_0 = \pi/2$ and $P = 0.71$, adopting a square solution domain, with various choices of the square side L, i.e., the position of the truncation limit, up to a value of 500.

Particular attention was given to the secondary boundary layer, where the asymptotic behavior represented by boundary-layer theory is approached less rapidly.

As an example of the variable-spacing grid automatically generated by the present method, the grid for the case $L = 100$ is reported in Fig. 6. As can be seen, the majority of the mesh points is packed close to the vertical wall because of the slight thickness of the vertical boundary layer; a much more moderate packing exists near the horizontal wall because the secondary boundary layer is much thicker, and the mesh is coarsest in the outer region far from both walls.

The streamlines and isothermal lines obtained in the calculation with $L = 100$ are shown in Fig. 7; the skin friction, i.e., the vorticity, on the secondary wall is shown in Fig. 8 on a logarithmic scale together with the theoretical boundary-layer prediction. While the streamlines clearly exhibit the shape sketched in Fig. 4 and the vertical boundary layer appears sharply defined, the secondary boundary-layer skin friction is still not close to the predicted asymptotic behavior.

Similar plots for a calculation performed with a square side of 500 appear in Figs. 9 and 10. (In Fig. 9, the isothermal lines are not plotted because they are too close to the vertical wall.) An improvement can be observed in the skin friction plot, where the difference from the asymptotic solution diminishes from 80% at $y = 100$ to 30% at $y = 500$. [This rather large error is justified by the relative thickness of the secondary boundary layer. In fact, it can be seen from Fig. 3 that at $z = 6$ velocity attains 90% of its asymptotic

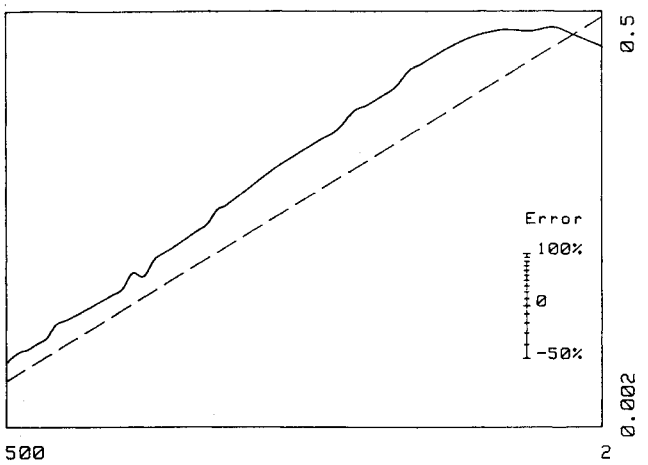

Fig. 10 Bilogarithmic plot of the second wall skin friction for $L=500$.

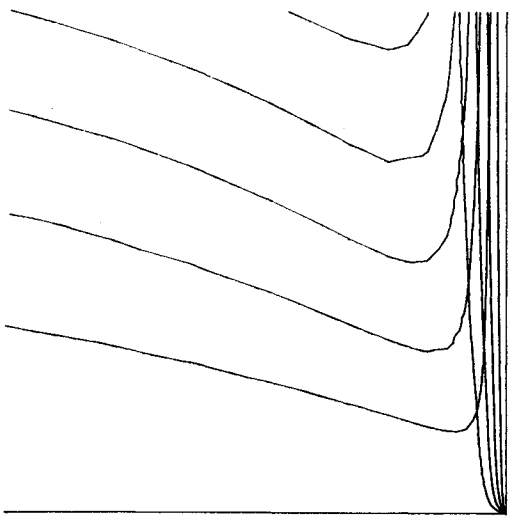

Fig. 11 Streamlines and isothermal lines in a 100×100 portion of the 500×500 calculation.

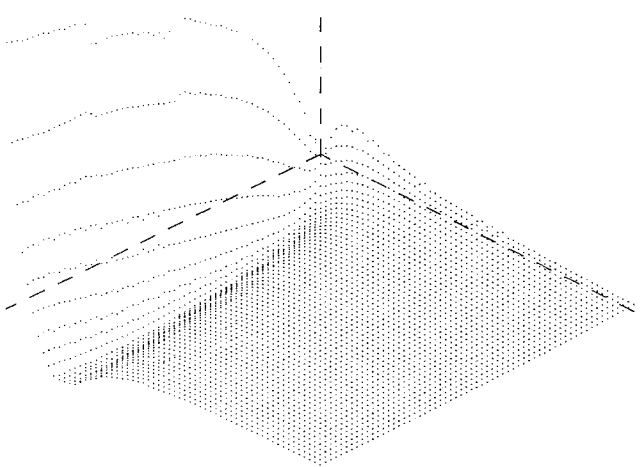

Fig. 12 Vorticity distribution in a 40×40 portion of the flowfield.

value. Choosing this limit as the boundary-layer edge, one finds that $y=\zeta x^{5/8}=6\cdot(500)^{5/8}\simeq290$.]

In both Figs. 7 and 9 the distortion of streamlines near the fake truncation boundary can be noticed. To show a streamline plot free of this effect, a 100×100 portion of the 500×500 solution is shown in Fig. 11. In this figure the typical behavior of the outer region can be well recognized.

Finally, Fig. 12 gives a three-dimensional plot of the vorticity distribution on a 40×40 portion of the flowfield, clearly showing the existence of the separate regions identified in the theoretical analysis, i.e., the two boundary layers and the outer region of null vorticity. It is also interesting to notice how the vorticity vanishes at the corner, in accordance with the solution of the Stokes equations.

V. Concluding Remarks

The analysis performed using the matched asymptotic expansions technique has revealed several interesting features of the natural convection flow in a corner, particularly concerning the character of the flowfield outside the thermal boundary layer.

Several distinct regions have been identified, giving exact solutions for the approximate equations valid in each of these regions. The vertical boundary layer has been found to be characterized by the classical similar solution, and to be the only region where thermal effects are present. In fact, temperature decreases exponentially going out of this boundary layer and is zero in all of the other regions. For the irrotational outer region a solution depending on the angle φ_0 between the two plates has been found, with the peculiar characteristic of becoming singular for an angle $\varphi_0=4\pi/3$. A solution of the infinite problem does not exist for angles greater than this limit, because the influence of the far portion of the heat source is not decreasing rapidly enough to allow the Green's function integral to converge.

For the secondary boundary layer formed on the second wall, a similar solution has been found such that the boundary-layer thickness decreases in the direction of the outer flow and the fluid goes out of the boundary layer into the outer region. This special behavior can be ascribed to the rapid increase of velocity in the streamwise direction.

A solution has also been found for the Stokes equations, describing the region very close to the corner.

The numerical solution of the full Navier-Stokes equations has been performed by a variable-spacing method devised by the present author for the case $\varphi_0=\pi/2$, confirming the validity of the scheme adopted in the theoretical analysis. To obtain an agreement between the numerical solution and the solution for the secondary boundary layer it has been necessary to extend the calculation to a very large domain due to the slow convergence of the boundary-layer approximation, which, in this case, can also be predicted theoretically. In light of the analysis performed, the observed error of 30% at $y=500$ is to be considered completely satisfactory.

Acknowledgment

This work was supported by the Consiglio Nazionale delle Richerche, Italy.

References

[1]Eckert, E. R. G. et al., "Heat Transfer—A Review of 1983 Literature," *International Journal of Heat and Mass Transfer*, Vol. 27, 1984, pp. 2179-2214.

[2]Lorentz, L., "Über das Leitungsvermogen der Metalle für Wärme und Electricität," *Wiedemanns Annalem*, Vol. 13, 1881, pp. 582-606.

[3]Schlichting, H., *Boundary Layer Theory*, McGraw Hill Book Co., New York, 1968, Sec. XIV.h.

[4]Brown, S. N. and Riley, N., *Journal of Fluid Mechanics*, Vol. 59, 1973, p. 225.

[5]Ingham, D. B., *International Journal of Heat and Mass Transfer*, Vol. 21, 1978, p. 67.

[6]Callahan, G. D. and Marner, W. J., *International Journal of Heat and Mass Transfer*, Vol. 19, 1976, p. 165.

[7]Soundalgekar, V. M. and Wavre, P. D., *International Journal of Heat and Mass Transfer*, Vol. 20, 1977, p. 1367.

[8]Yao, L. S., "Free and Forced Convection in the Entry Region of a Heated Vertical Channel," *International Journal of Heat and Mass Transfer*, Vol. 26, 1983, pp. 65-72.

[9]Yang, K. T. and Jerger, E. N., "First-Order Perturbations of Laminar Free-Convection Boundary Layers on a Vertical Plate,"

ASME Transactions, Journal of Heat Transfer, Vol. 86, 1964, pp. 107-115.

[10]Kishinami, K. and Seki, N., "Natural Convection Heat Transfer on an Unheated Vertical Plate Attached to an Upstream Isothermal Plate," *ASME Transactions, Journal of Heat Transfer*, Vol. 105, 1983, p. 759.

[11]Sparrow, E. M., Patankar, S. V., and Abdel-Wahed, R. M., "Development of Wall and Free Plumes Above a Heated Vertical Plate," *ASME Transactions, Journal of Heat Transfer*, Vol. 100, 1978, pp. 184-190.

[12]Luchini, P. and Pozzi, A., "High Prandtl Number Free Convection Beside and Above a Heated Vertical Plate," *Proceedings of the VII AIMETA Conference*, Trieste, Italy, Oct. 1984, pp. 165-175.

[13]Kierkus, W. T., "An Analysis of Laminar Free Convection Flow and Heat Transfer About an Inclined Isothermal Plate," *International Journal of Heat and Mass Transfer*, Vol. 11, 1968, pp. 241-253.

[14]Na, T. Y. and Pop, I., "Free Convection Flow Past a Vertical Flat Plate Embedded in a Saturated Porous Medium," *International Journal of Engineering Science*, Vol. 21, 1983, p. 517.

[15]Clarke, J. F., "Transpiration and Natural Convection: The Vertical-Flat-Plate Problem," *Journal of Fluid Mechanics*, Vol. 57, 1973, pp. 45-61.

[16]Riley, N., "Note on a Paper by Kierkus," *International Journal of Heat and Mass Transfer*, Vol. 18, 1975, pp. 991-993.

[17]Rodighiero, C. and de Socio, L. M., "Some Aspects of Natural Convection in a Corner," *ASME Transactions, Journal of Heat Transfer*, Vol. 105, 1983, p. 212.

[18]Luchini, P., Pozzi, A., and de Socio, L., "Convezione naturale in un angolo," *Atti 37° Congresso Nazionale ATI*, Padova, Sept. 1982, pp. 615-622.

[19]Luchini, P., "An Adaptive-Mesh Finite-Difference Solution Method for the Navier-Stokes Equations," submitted to *Journal of Computational Physics*.

[20]Kuiken, H. K., "An Asymptotic Solution for Large Prandtl Number Free Convection," *Journal of Engineering Mathematics*, Vol. 2, 1968, pp. 355-379.

[21]Roache, J. P., *Computational Fluid Dynamics*, Hermosa Publishers, Albuquerque, NM, 1976. Sec. III-C.